

# Picosecond Molecular Motions in Bacteriorhodopsin from Neutron Scattering

J. Fitter,\*\* R. E. Lechner,\* and N. A. Dencher#

\*Hahn-Meitner-Institut, BENSC (NI), D-14109 Berlin, and #Institut für Biochemie, TU Darmstadt, D-64287 Darmstadt, Germany

**ABSTRACT** The characteristics of internal molecular motions of bacteriorhodopsin in the purple membrane have been studied by quasielastic incoherent neutron scattering. Because of the quasihomogeneous distribution of hydrogen atoms in biological molecules, this technique enables one to study a wide variety of intramolecular motions, especially those occurring in the picosecond to nanosecond time scale. We performed measurements at different energy resolutions with samples at various hydration levels within a temperature range of 10–300 K. The analysis of the data revealed a dynamical transition at temperatures  $T_d$  between 180 K and 220 K for all motions resolved at time scales ranging from 0.1 to a few hundred picoseconds. Whereas below  $T_d$  the motions are purely vibrational, they are predominantly diffusive above  $T_d$ , characterized by an enormously broad distribution of correlation times. The variation of the hydration level, on the other hand, mainly affects motions slower than a few picoseconds.

## INTRODUCTION

Biological macromolecules, such as enzymes or transport proteins, share a structural complexity, which is also reflected in a complex dynamical behavior. The large number of polypeptide side groups and the superposition of reorientational motions of these groups yield a remarkably rich dynamical spectrum ranging from rapid local vibrations to slow collective distortions of large domains within the protein. These internal motions are characterized by correlation times from  $10^{-14}$  to  $10^1$  s (McCammon and Harvey, 1987). Dynamical properties of biological macromolecules, particularly proteins, have been studied with various experimental and theoretical methods (see, for example, Rupley and Careri, 1991; McCammon and Harvey, 1987). Neutron spectroscopy using time-of-flight and backscattering spectrometers permits the investigation of motions in the time range from  $10^{-13}$  to  $10^{-9}$  s. On this time scale the spectrum is dominated by various types of thermal fluctuations from small-amplitude internal vibrations up to large-amplitude diffusive reorientational motions of molecular subunits (e.g., polypeptide side groups). In particular, the quasielastic incoherent neutron scattering (QINS) of hydrogen atoms reveals some important dynamical properties of biological macromolecules, because this technique resolves both structural and dynamical details at the molecular scale (Lechner, 1983). Because of the large incoherent cross section of hydrogen nuclei ( $\sim 40$  times larger than the cross section of other elements) and the fact that hydrogen atoms are distributed nearly homogeneously in a biological macromolecule, this technique is a powerful tool for the study of all internal motions.

The temperature as well as the hydration are of outstanding importance for the dynamical behavior of biological macromolecules. This is indicated by the fact that proteins in general are “fully functional” only under physiological temperatures and at a sufficient hydration level. The study of the dynamical characteristics as a function of these parameters may give information about the kind of dynamical properties that are essential for the function. Recent studies using neutron scattering and Mössbauer spectroscopy investigated the temperature dependence of protein dynamics in fully hydrated as well as in “dry” samples of globular, water-soluble proteins (Parak et al., 1982; Doster et al., 1989; Andreani et al., 1995). Because of phenomenological similarities between proteins and glass-forming liquids, the observations in these studies have been related to the well-known dynamical glass transition (Iben et al., 1989), which occurs in proteins at temperatures between 180 and 230 K. Below this temperature mainly vibrational motions and correspondingly small global average mean square displacements are observed. Above the transition temperature, the motions in fully hydrated samples become more and more anharmonic and even have the character of diffusive motions, resulting in much larger mean square displacements. “Dry” samples show only a small increase in mean square displacements at temperatures above the transition temperature.

As a prominent prototype of an active transport protein, we have investigated the membrane protein bacteriorhodopsin (BR) by using QINS. BR, which serves as a light-driven proton pump in *Halobacterium salinarum*, is the only protein in the purple membrane (PM) and aggregates with a few lipids into a highly ordered two-dimensional lattice. BR shares with many other membrane proteins the seven-helix structure, which has been studied extensively by cryoelectron microscopy (Henderson et al., 1990; Grigorieff et al., 1996). The application of many biophysical methods demonstrated that BR is an appropriate candidate for extending our knowledge of the structure-function relation of proteins

Received for publication 18 February 1997 and in final form 18 June 1997.

Address reprint requests to Dr. Joerg Fitter, Hahn-Meitner-Institut, BENSC (NI), Glienicke Strasse 100, D-14109 Berlin, Germany. Tel.: 49-30-8062-3073; Fax: 49-30-8062-2999; E-mail: fitter@hmi.de.

© 1997 by the Biophysical Society

0006-3495/97/10/2126/12 \$2.00

(Dencher et al., 1989; Koch et al., 1991; Hauss et al., 1994; Sass et al., 1997). Thermal fluctuations of BR on the pico-second time scale have been studied as a function of temperature by incoherent neutron scattering (INS) in work by Ferrand and co-workers (1993).

In recent QINS studies we investigated the dynamical behavior of hydration water (Lechner et al., 1994a, b) on PM, as well as the protein dynamics of BR (Fitter et al., 1995, 1996b). These studies were performed with samples at room temperature, and we focused our analysis on the interpretation of the data by using specific models. The subject of the present work is a QINS study as a function of temperature (10 K to 300 K) of PM samples hydrated with D<sub>2</sub>O at several different levels. The effects of temperature and hydration on the dynamics of the protein-lipid complex were examined by a phenomenological analysis. This analysis makes use of the concept of quasielastic incoherent structure factors (Lechner, 1994) to quantify the internal flexibility within the PM and its dependence on environmental conditions.

## MATERIALS AND METHODS

### Samples

Purple membrane sheets were isolated from *H. salinarum* and washed with distilled water. In addition to the natural PM, with a lipid content of ~25% (w/w) (Kates et al., 1982), we prepared delipidated PM with only 5% (w/w) lipids. Lipids were partially removed from PM without BR solubilization by a method that has been described in detail elsewhere (Fitter et al., 1996a). A suspension of 300 mg natural or delipidated PM, respectively, was deposited on planar aluminum foil and was dried in an exsiccator. With relatively slow drying over 3 days we obtained PM stacks with membrane planes parallel to the surface of the aluminum foil. Then the samples were rehydrated with D<sub>2</sub>O and equilibrated at different hydration levels, using vapor exchange over pure D<sub>2</sub>O and over saturated salt solutions to achieve specific relative humidities (see, for example, Landolt-Börnstein, 1967) inside the exsiccator. Relative humidities from 10% to 100% were used, which corresponded to hydration levels ranging from 0.05 to 0.56 g D<sub>2</sub>O/g PM. The various hydration levels were reached within 3 days. The samples were made of alternating layers of solvent water molecules and PM sheets, giving them the character of lamellar structures. The hydration level of the samples was controlled by the determination of the sample weight as well as the lamellar spacing. The latter was obtained from neutron diffraction experiments. Finally, the equilibrated samples were sealed in a circular slab-shaped aluminum container, which protected the samples against the dry helium atmosphere inside the cryostat at the spectrometer.

### Measurements

The experiments were carried out using the time-of-flight spectrometers NEAT (HMI, Berlin) and IN6 (ILL, Grenoble) and the backscattering

spectrometer IN10 (ILL, Grenoble). The relevant spectrometer characteristics as well as the spectrometer settings that were used during the measurements are shown in Table 1. All samples, including vanadium standard and empty can, were measured with a sample orientation angle of  $\alpha = 45^\circ$  with respect to the incident neutron beam direction. The different temperatures were achieved within an experimental error limit of  $\pm 1$  K by using a cryostat, which was the same ILL standard type (orange cryostat) at all spectrometers. Between 200 and 300 K a step width of 10 K was used, and below 200 K we measured only at a few temperatures. More methodical details have been published elsewhere (Lechner et al., 1994a; Fitter et al., 1995).

### Incoherent neutron scattering

We are dealing with incoherent neutron scattering, and the predominant part of the measured signal is due to nonexchangeable hydrogen atoms. Most of the polar and charged polypeptide side groups as well as the polar lipid headgroups contain exchangeable protons, which are replaced by deuterons if the samples are hydrated with D<sub>2</sub>O. Nevertheless, most of the protons are not exchangeable and, from a practical point of view relevant for the QINS analysis, these protons are distributed nearly homogeneously in the sample (see Table 2). In contrast to small-angle neutron scattering (SANS) techniques and other neutron diffraction methods, we are not dealing with H/D contrast matching, because we do not have scattering from Bragg reflections, and we do not include data from small scattering angles (within the studied range of scattering angles and with  $\alpha = 45^\circ$ ). For this reason we have to consider the same individual incoherent cross section for all hydrogens (79.91 barns), which "monitor" the general dynamical properties of the sample as a probe. In this case the double-differential cross section,

$$\frac{\partial^2 \sigma}{\partial \Omega \partial \omega} = \frac{1}{4\pi} \cdot \frac{|\vec{k}_1|}{|\vec{k}_0|} \cdot b_{\text{inc}}^2 \cdot S_{\text{inc}}(\vec{Q}, \omega) \quad (1)$$

determines the number of neutrons scattered into a solid angle element  $\partial \Omega$  and an energy transfer element  $\partial \omega$ . The wave vectors for incident and scattered neutrons are given by  $\vec{k}_0$  and  $\vec{k}_1$ , respectively, and  $b_{\text{inc}}$  is the incoherent scattering length. Using the formalism of self-correlation functions developed by Van Hove (1954), the incoherent scattering function  $S_{\text{inc}}(\vec{Q}, \omega)$  can be related to the self-correlation function  $G_s(\vec{r}, t)$ :

$$S_{\text{inc}}(\vec{Q}, \omega) = \frac{1}{2\pi} \int_{-\infty}^{\infty} e^{-i\omega t} \int_{-\infty}^{\infty} e^{i\vec{Q}\vec{r}} \cdot G_s(\vec{r}, t) d\vec{r} dt \quad (2)$$

Here  $G_s(\vec{r}, t)$  is the Fourier transform in space and time of the incoherent scattering function. In the classical approximation,  $G_s(\vec{r}, t)$  describes the average time-dependent probability density distribution of hydrogen atoms (see, for example, Lechner, 1983).

### Data analysis

The measured time-of-flight (TOF) spectra were corrected, normalized, and transformed to the energy transfer scale by adapted standard routines. At the present stage of our data analysis, the spectra were not corrected for

**TABLE 1** Spectrometer characteristics and settings applied for the measurements

	NEAT	IN6	IN10
Elastic wavelength $\lambda_e$	5.10 Å	5.12 Å	6.271 Å
Angular range $\phi$	13.3–136.7°	10.3–113.5°	14.3–153.23°
Elastic energy resolution (FWHM)	100 $\mu$ eV	80 $\mu$ eV	1.8 $\mu$ eV
Energy transfer range	–2.2–8.0 meV	–2.0–8.0 meV	$\pm 0.015$ meV

**TABLE 2** Number of protons per BR molecule

	Natural PM		Delipidated PM	
	Nonexchangeable	Exchangeable	Nonexchangeable	Exchangeable
BR	1891	78	1891	78
Lipids	635	35	127	7
PM	2526	113	2018	85

In addition to nonexchangeable protons (mostly carbon bound), there are also exchangeable protons, which are generally replaced by deuterons if the samples are hydrated with D<sub>2</sub>O. Structural information of the lipid molecules (Kates et al., 1982) and of BR (Ovchinnikov et al., 1979) has been used to calculate the given numbers.

multiple scattering, because we performed measurements with sample transmissions of ~90–95%. The spectra measured with the time-of-flight spectrometers NEAT and IN6, characterized by a rather large energy transfer range, have been transformed and binned to constant  $Q$  (momentum transfer) spectra. Using the energy transfer ranges given in Table 1, six spectra with  $Q$  values ranging from 1.2 to 1.7 Å<sup>-1</sup> were obtained. To study the average thermal fluctuation within the protein-lipid complex as a function of environmental conditions, in the present analysis we did not use specific models, but a phenomenological fitting procedure. The following scattering function  $S_{PM}(\vec{Q}, \omega)$  was applied to describe the dynamical behavior of the PM:

$$S_{PM}(\vec{Q}, \omega) = e^{-(\omega^2)Q^2} \cdot [\text{EISF}(\vec{Q}) \cdot \delta(\omega) + \sum_n \text{QISF}_n(\vec{Q}) \cdot L_n(H_n, \omega)] \quad (3)$$

This type of expression (see Lechner, 1994) permits a model-independent separation of the scattered intensity into an elastic  $\delta(\omega)$ -shaped component and quasielastic Lorentzian-shaped contributions  $L_n(H_n, \omega)$ , where  $H_n = (\tau_n)^{-1}$  are the widths (half-width half-maximum) of the Lorentzians ( $\tau_n$  are the corresponding correlation times). The elastic scattering amplitude is described by the elastic incoherent structure factor (EISF) and the quasielastic scattering amplitudes by  $n$  quasielastic incoherent structure factors (QISF<sub>*n*</sub>). Although predominant scattering was due to hydrogens located in the protein-lipid complex, scattering of deuterons, mainly from D<sub>2</sub>O solvent, is still a few percent, depending on the hydration level. In previous publications we have already analyzed the dynamical behavior of hydration water on purple membranes, so that we may approximate the scattering of D<sub>2</sub>O molecules by a properly weighted term developed for H<sub>2</sub>O molecules (Lechner et al., 1994a, b). In these previous studies we described the motions of water molecules by a specific model, which took into account translational diffusion ( $S_{\text{trans}}(\vec{Q}, \omega)$ ) and rotational diffusion ( $S_{\text{rot}}(\vec{Q}, \omega)$ ), resulting in the following convolution expression:

$$S_{\text{sol}}(\vec{Q}, \omega) = S_{\text{rot}}(\vec{Q}, \omega) \otimes S_{\text{trans}}(\vec{Q}, \omega) \quad (4)$$

According to this model, the quasielastic structure factor QISF<sub>*r*</sub> of  $S_{\text{rot}}(\vec{Q}, \omega)$  (with width  $H_r$ ) has been used to describe the quasielastic scattering of rotational diffusion and the quasielastic structure factor QISF<sub>*t*</sub> of  $S_{\text{trans}}(\vec{Q}, \omega)$  (with width  $H_t$ ) for the translational diffusion. The values of these parameters have been taken from previous work (Fitter, 1994; Lechner et al., 1994b) and are given in the legend of Fig. 2 in the next section. At temperatures below  $T_f$  (see next section), we assumed the scattering due to solvent molecules to be purely elastic.

The scattering intensities from the PM and the solvent have been considered by a statistical weight  $F$  for each category (the sum of all  $F$ 's is equal to unity), which gives a resulting theoretical scattering function:

$$S_{\text{theor}}(\vec{Q}, \omega) = F_{PM} \cdot S_{PM}(\vec{Q}, \omega) + F_{\text{sol}} \cdot S_{\text{sol}}(\vec{Q}, \omega) \quad (5)$$

The value for the statistical weight  $F_{\text{sol}}$  is proportional to the hydration  $h$  and shows that the scattering from solvent molecules ranges from 0.4% to 5% of the total scattering, depending on the hydration level. (The statistical weight reads  $F_{\text{sol}} = h \cdot SP_D$ , where  $SP_D = 1/11$  is the scattering power of

deuterons compared to that of hydrogens.) The scattering from the protein-lipid complex is mainly due to the nonexchangeable hydrogens of the PM (see Table 2). Because we are not able to distinguish between scattering from the lipids and that from the protein, the dynamical properties of both will be analyzed together in the components of  $S_{PM}(\vec{Q}, \omega)$ . On the other hand, the numbers of protons located in the protein and the lipids (Table 2) show that scattering from the protein is dominating the spectra. With respect to the dry PM (i.e., without solvent), the contribution of scattering from BR is 75% in the case of natural PM and 94% in the case of delipidated PM.

We fit the theoretical scattering function to the measured  $S_{\text{meas}}(\vec{Q}, \omega)$  scattering function by using

$$S_{\text{meas}}(\vec{Q}, \omega) = F_N \cdot e^{-\hbar\omega/2k_B T} \cdot [S_{\text{theor}}(\vec{Q}, \omega) \otimes S_{\text{res}}(\vec{Q}, \omega)] \quad (6)$$

Here  $F_N$  represents a normalization factor,  $e^{-\hbar\omega/2k_B T}$  is the detailed balance factor, and  $S_{\text{res}}(\vec{Q}, \omega)$  is the resolution function obtained from vanadium measurements, which is convoluted ( $\otimes$ : energy convolution operator) with the theoretical scattering function.

At the present stage of the analysis we focus mainly on results obtained at only one relatively large value of momentum transfer ( $Q = 1.7$  Å<sup>-1</sup>). The analysis of data within a relatively large energy transfer range requires constant  $Q$  data (although the spectra have been measured at constant scattering angle  $\phi$ ), because  $Q$  is not only a function of  $\phi$ , but also a function of the energy transfer  $\omega$ . Considering the fact that we are dealing with combined data from different instruments, 1.7 Å<sup>-1</sup> was the largest available value of  $Q$ . Furthermore, we observed at this  $Q$  value the largest amplitudes from quasielastic scattering, as compared to smaller  $Q$  values. In this sense the value of  $Q = 1.7$  Å<sup>-1</sup> is the most suitable one for the analysis of effects like dependence on temperature and on hydration level, because the QISF values at this momentum transfer may be considered as expressive parameters quantifying a "general flexibility" within the protein-lipid complex. A report on an analysis focusing on the spatial information of PM dynamics ( $Q$  dependence) contained in the experimental data will be postponed to a later publication (Fitter et al., manuscript in preparation).

## PROPERTIES OF THE MEASURED TOF SPECTRA OF PM

As already mentioned in the previous section, we measured spectra with different elastic energy resolutions. To characterize the scattering occurring from the protein-lipid complex, we first performed a purely phenomenological fit, based on Eq. 3 (and setting  $S_{\text{sol}}(\vec{Q}, \omega) = 0$  in Eq. 5), of spectra measured at room temperature. It revealed the following features:

1. All spectra measured with the specific elastic energy resolutions ( $\Delta E = 1.8, 80, \text{ and } 100 \mu\text{eV}$  (full width half-maximum) can be fit with two quasielastic components. In

these fits linewidths and structure factors of both components have been used as free parameters. Applying fits with more quasielastic components does not significantly improve the quality of fits within their individual energy transfer ranges. Fits with two quasielastic components revealed that the spectra can be decomposed into a rather broad component with a linewidth of a few meV and a second component with a linewidth strongly correlated with the resolution width. The linewidth of the latter component is larger by a factor of 2 or 3, as compared with the resolution width (see Fig. 1 and Table 3).

2. The integral of the quasielastic incoherent scattering increases from small to large  $Q$  values.

3. The obtained linewidths do not show a significant  $Q$  dependence.

4. An increase in the total quasielastic scattering is observed when going from lower to higher energy resolution (100 to 1.8  $\mu\text{eV}$ ) (Table 3). The fact that we obtain different average linewidths, even for only slightly different energy resolutions (see  $H_2$  for NEAT and IN6 in Table 3), is a strong indication that the quasielastic spectrum of purple membranes could also be described by a large number of

Lorentzians showing a broad and more or less continuous distribution of linewidths. The linewidths obtained at specific energy resolutions must be understood as mean values of a distribution of linewidths, and the related motions are characterized by the corresponding range of different correlation times. The elastic energy resolution as well as the energy transfer range determine which part of this wide distribution of linewidths is singled out by the measurement. (In this sense a linewidth obtained from the fit is not only a sample property, but also a distinct feature of the spectrometer setting.) Furthermore, a clear distinction between vibrational and diffusive motions within the measured spectra is not possible in every case. In particular, the broad Lorentzian-shaped components include contributions of vibrational motions (see next section, Fig. 3 C). As shown in recent studies, the major part of the scattering described by these components is due to local diffusive motions of hydrogen atoms within restricted volumes (with a size of a few  $\text{\AA}$ ) with correlation times from 0.1 to 200 ps (Fitter et al., 1995, 1996b). Stochastic reorientations of molecular subunits, such as methyl and larger polypeptide side groups are candidates for this kind of motion. The very

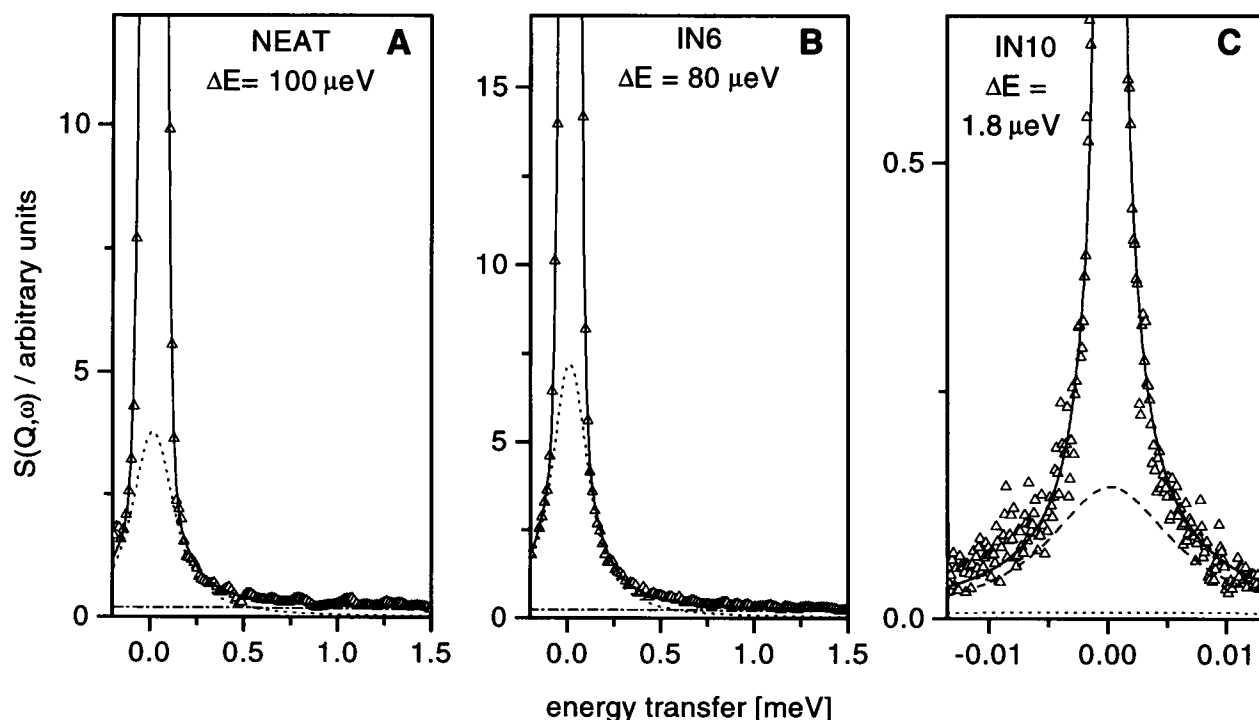


FIGURE 1 A comparison of spectra measured with delipidated, fully hydrated PM [0.38 g  $\text{D}_2\text{O/g PM}$ ]. These room-temperature measurements have been performed at a momentum transfer of  $Q = 1.7 \text{ \AA}^{-1}$ , using three different energy resolutions ( $\Delta E$  in [FWHM]). For the purpose of comparison the intensity scale has been chosen such that the highest value shown (top of frame) is 20% of the elastic peak intensity in each case. The spectra measured with NEAT and IN6 have been fitted with two quasielastic components, whereas three quasielastic components have been applied in the case of IN10 data. This figure shows the total scattering function (solid line) fitting the experimental points (triangles). The Lorentzian-shaped quasielastic contribution  $L_1$  is represented by the dashed-dotted line,  $L_2$  by the dotted line, and  $L_3$  by the dashed line (only IN10). The obtained linewidths and quasielastic incoherent structure factors are given in Table 3. Note that two quasielastic components can fit all spectra with a sufficient quality within their energy transfer range. Nevertheless, we applied an additional third quasielastic component in the case of IN10 spectra. Because of the small energy transfer range of IN10 data, the still existing "broader" components cannot be determined precisely. Therefore, we included both quasielastic components ( $L_1$ ,  $L_2$ ) with structure factors and linewidths obtained from the NEAT spectra as "fixed numbers." This procedure enabled us to compare the total quasielastic scattering (see Table 3) of spectra measured at very different elastic energy resolutions.

**TABLE 3** The parameters characterizing the quasielastic contribution are given for the fits of spectra measured with three different energy resolutions

Quasielastic contribution	$L_1$		$L_2$		$L_3$		Total QISF QISF <sub>3</sub>
	$H_1$ [meV]	QISF <sub>1</sub>	$H_2$ [ $\mu$ eV]	QISF <sub>2</sub>	$H_3$ [ $\mu$ eV]	QISF <sub>3</sub>	
NEAT	4.0	0.27	113.50	0.164	—	—	0.434
IN6	3.9	0.26	102.07	0.211	—	—	0.471
IN10	4.0	0.27	113.50	0.164	5.88	0.198	0.632

The quasielastic structure factors and the corresponding linewidths of the components  $L_1$  and  $L_2$  have been used as free fitting parameters in the case of NEAT and IN6 data. In the case of IN10 data, only the parameters of  $L_3$  were free in the fitting procedure, whereas the parameters of  $L_1$  and  $L_2$  have been taken from NEAT spectra and were used as fixed parameters. See Fig. 1.

slow motions contribute “elastic scattering” to the spectra, measured at low energy resolution, but occur as quasielastic scattering (and thus increase the total QISF) in spectra measured at higher energy resolution. The large number of different polypeptide side groups and other molecular subunits as parts of the protein-lipid complex and their individual motions are responsible for this enormous variety in the dynamical behavior (see also Parak et al., 1993).

## THE TEMPERATURE DEPENDENCE

We performed measurements at temperatures ranging from 100 K to 300 K (respectively, from 10 K to 300 K) at those three different elastic energy resolutions (see Table 1). Phenomenological fits as described in the previous section have been applied to all measured spectra. Just as in the case of spectra measured at room temperature, spectra from measurements at lower temperatures can be fitted with only two Lorentzians. Here also, every Lorentzian represents a broad distribution of many Lorentzians, each characterized by its own linewidth. As a consequence of this, there is a strong correlation between the values of the fit parameters (quasielastic structure factors and linewidths), and this makes the analysis of the temperature effects more difficult. The minimum of the sum of error squares in the least-squares fitting procedure turns out to be very flat. Therefore there is appreciable uncertainty in the determination of  $H$  and QISF, characterized by correlated pairs of strongly fluctuating individual parameter values. Nevertheless, to obtain a smooth phenomenological description of the temperature dependence, the following method was applied.

First the quasielastic structure factors and their corresponding linewidths were determined from spectra measured at room temperature. Then the data taken at other temperatures were examined:

1. Fits at lower temperatures were performed with fixed linewidths (obtained from room-temperature fits), but with structure factors as free parameters.

2. Fits at lower temperatures were performed with fixed structure factors (obtained from room-temperature fits), but with linewidths as free parameters.

Both kinds of procedures give fitting results of the same acceptable quality. Furthermore, both procedures revealed the main features of the temperature dependence (presented

below in the section Quasielastic structure factors). The general decrease in quasielastic scattering, which is present from the phenomenological point of view in both 1 and 2, may be due to one of several possible, qualitatively different dynamical properties. The decrease can be caused by a reduction in jump distances (smaller volume explored by the moving unit), by a reduction in jump rates (slowing of the motion), or a combination of both. Any of these may lead to a partial or complete disappearance of the diffusive motions (“freeze out”). In the case of a complex dynamical behavior such as that observed in biological macromolecules, it is not always possible to distinguish between the various above-mentioned alternatives.

## Crystallization and supercooling of solvent molecules in PM samples

Although the study of dynamical aspects of the hydration water is not within the focus of this study, some solvent properties are of fundamental interest, because they are correlated with the dynamical properties of the protein-lipid complex (see, for example, Rupley and Careri, 1991). In the case of PM samples, solvent molecules are located in the interior of the protein, on the surface of the protein and lipid molecules, as well as in the interbilayer space between two adjacent PM fragments. Because of the geometry of the PM fragments, most of the solvent molecules are located in the interbilayer space if the samples are hydrated above a level of  $h = 0.05$  g D<sub>2</sub>O/g PM. (Compared to BR molecules, which are embedded in a lipid bilayer, water-soluble proteins need many more solvent molecules to cover the whole surface of the protein.) At relatively high hydration levels ( $h = 0.3$  g D<sub>2</sub>O/g PM), the water molecules undergo a long-range translational diffusion parallel to the membrane surface, characterized by a room-temperature diffusion coefficient of  $D_s = 4.4 \cdot 10^{-6}$  cm<sup>2</sup>/s, which is about five times slower than that of bulk water (Lechner et al., 1994b). At lower hydration levels ( $h = 0.05$  g D<sub>2</sub>O/g PM) such a translational diffusion was not observed. As known from previous studies, it is possible that hydration water does not crystallize at low temperatures (Kuntz and Kauzmann, 1974; Doster et al., 1986). The conditions for supercooling of water molecules depend on the hydration level and on the geometry of the surface of the biological macromolecules.

To achieve supercooling, it seems to be of importance that the water molecules interact strongly with the biological macromolecule (Rupley and Careri, 1991).

Concerning crystallization and supercooling of solvent water in PM samples, we observed the following:

TOF spectra measured with NEAT and IN6 clearly show Bragg peaks due to ice in the case of PM samples hydrated at levels above  $h = 0.18$  g D<sub>2</sub>O/g PM. The fact that these Bragg peaks occur only at temperatures  $T_f$  below 267 K indicates that hydration water is supercooled down to this temperature.

At high hydration levels, the major part of the solvent water is located in the interbilayer space and participates in crystallization below the freezing temperature  $T_f$ . Those solvent molecules that crystallize cannot contribute in the usual sense to the hydration of the protein-lipid complex. Therefore the "effective" hydration level is reduced at temperatures below  $T_f$ . The crystallization of hydration water at low temperatures was observed in PM samples at hydration levels down to at least 0.2 g D<sub>2</sub>O/g PM. Details of these observations are reported in another publication (Lechner et al., manuscript submitted for publication).

### Quasielastic structure factors

The investigation of an average internal molecular flexibility within the PM-protein-lipid complex was realized by the determination of the quasielastic structure factors as a function of temperature. Fits of spectra measured at the different temperatures have been performed, using fixed values for the linewidths as obtained from fits of spectra measured at room temperature. The temperature dependence of the resulting quasielastic incoherent structure factors, as determined in fits of spectra measured with fully hydrated delipidated PM samples, is shown in Figs. 2 and 3. For one elastic energy resolution (NEAT  $\Delta E = 100$   $\mu$ eV), we have also performed measurements of the delipidated sample at low hydration level. As shown in a recent study (Fitter et al., 1997), we know that the protein/lipid ratio in the PM has an influence on the dynamical behavior of the protein-lipid complex. Therefore, in addition we measured a fully hydrated natural PM as a function of temperature. The analysis of these measurements yielded the following results:

1. Combining the results of measurements performed with three different elastic energy resolutions, we were able to separate three different quasielastic components with their individual structure factors (QISF<sub>1</sub> – QISF<sub>3</sub>) and average linewidths (corresponding correlation times):  $H_1 = 4.0$  meV ( $\tau_1 = 0.16$  ps),  $H_2 = 110$ – $120$   $\mu$ eV ( $\tau_2 = 6.0$ – $5.5$  ps), and  $H_3 = 5.5$   $\mu$ eV ( $\tau_3 = 120$  ps). (The relation between linewidths and correlation times, as defined in our phenomenological treatment, reads:  $\tau[\text{sec}] = (H[\text{meV}] \cdot 1.519 \cdot 10^{12})^{-1}$ .)

2. The "slowest" component, represented by QISF<sub>3</sub>, decreases in the temperature range from 300 K to 200 K. We do not find an appreciable contribution of this component below a temperature of  $\sim 180$ – $220$  K (Fig. 3 A).

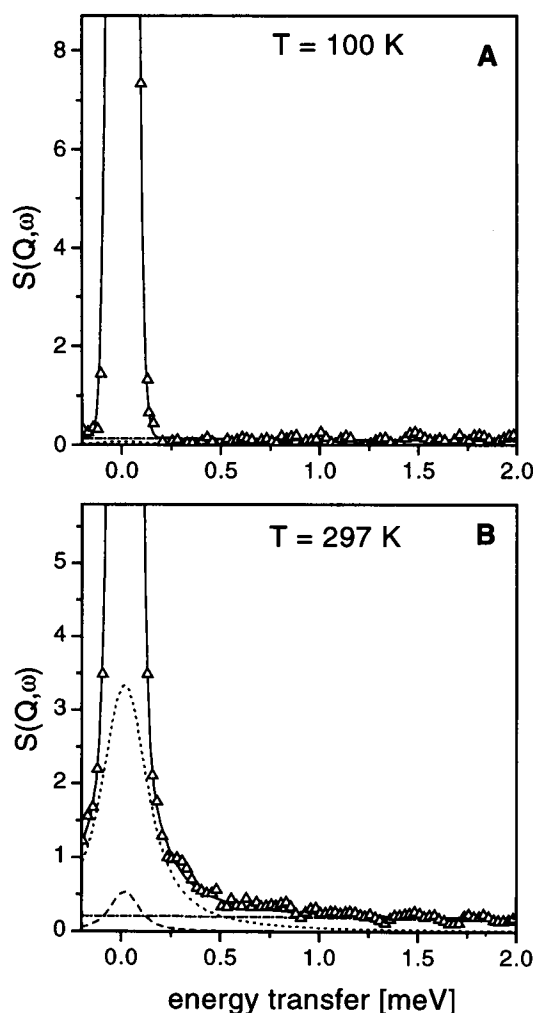


FIGURE 2 As an example of the temperature dependence, fits of NEAT spectra ( $Q = 1.7$   $\text{\AA}^{-1}$ ) measured at two different temperatures (a: 100 K; b: 297 K) are shown. The total scattering function (solid line), which fits the experimental points (triangles), includes the following quasielastic components: scattering from the PM, represented by Lorentzian  $L_1$  with  $H_1 = 4$  meV (dashed-dotted line), and  $L_2$  with  $H_2 = 120$   $\mu$ eV (dotted line). Scattering due to rotational diffusion of D<sub>2</sub>O molecules is represented by  $L_r$ , with QISF<sub>r</sub> = 0.4 and  $H_r = 60$   $\mu$ eV (dashed line). Quasielastic scattering due to translational diffusion of solvent molecules ( $H_t = 7$   $\mu$ eV) is not resolved in the NEAT spectra and is therefore contained in the elastic component. The highest intensity values (top of the frame) shown in both figures correspond to 10% of the elastic peak intensity.

3. QISF<sub>2</sub>, representing motions characterized by correlation times of a few picoseconds, shows a gradual decrease with decreasing temperature. We find a moderate decrease between 300 K and 270 K, which is followed by a more pronounced decrease between 270 K and 260 K. From 250 K down to 200 K, we find again a moderate decrease, and below  $\sim 200$  K there is no significant scattering corresponding to this quasielastic contribution (Fig. 3 B).

4. The quasielastic component QISF<sub>1</sub>, representing "faster" motions, also shows a strong decrease in the temperature range from 300 K to 200 K. In contrast to the other components, QISF<sub>1</sub> still has an amplitude below 200 K, which

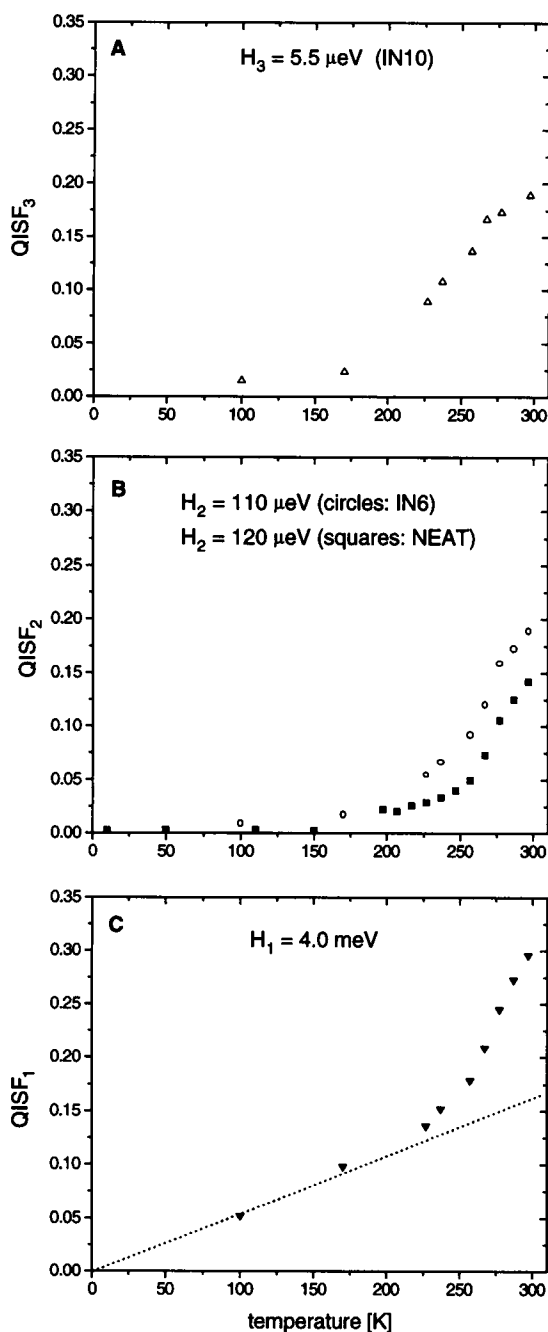


FIGURE 3 The temperature dependence of all quasielastic incoherent structure factors ( $\text{QISF}_1 - \text{QISF}_3$ ): for component  $L_3$  with corresponding correlation time  $\tau_3 = 120$  ps (a),  $L_2$  with  $\tau_2 = 6.0$  ps (IN6) and  $5.5$  (NEAT) (both b), and  $L_1$  with  $\tau_1 = 0.16$  ps (c). The dotted straight line in c represents a linear decrease in  $\text{QISF}_1$  at temperatures below  $200$  K, indicating vibrational motions in this temperature regimen (see also Fig. 4). The error of the given QISF values is about  $\pm 0.015$  at low temperatures (below  $200$  K), but is smaller at higher temperatures.

decreases less steeply and tends toward zero at  $0$  K, showing a temperature dependence typical for (more or less harmonic) vibrational motions (Fig. 3 C). This behavior is also confirmed by an "elastic-scan" measurement with IN10. From this measurement average mean square displace-

ments, including all motions with correlation times below  $\sim 300$  ps (limited by the instrument energy resolution), have been determined as a function of temperature (Fig. 4).

5. The quasielastic scattering obtained from spectra measured with weakly hydrated samples is much smaller in the temperature range from  $300$  K to  $262$  K (the latter is approximately the value of  $T_f$ ) compared to that obtained from fully hydrated samples. Below  $T_f$ ,  $\text{QISF}_2$  shows no significant difference between the two hydration levels (Fig. 5 A).

6. Comparing delipidated and natural PM, we find larger  $\text{QISF}_2$  values in the case of natural PM at high temperatures. This difference vanishes with decreasing temperatures, and we even find smaller values of  $\text{QISF}_2$  from the natural PM as compared to the delipidated PM at temperatures below  $T_f$ . Although the latter may be an interesting phenomenon, we are not able to analyze it in more detail, because we measured the natural PM only at two temperatures below  $T_f$ . Nevertheless, the general features of the temperature dependence, mainly described in result 3, are qualitatively observed for both types of samples, the delipidated and the natural PM one (Fig. 5 B).

The main feature of the investigated temperature dependence is characterized by a general reduction of thermal fluctuation with decreasing  $T$ , which is observed in the whole time scale, from a few hundred to a few tenths of picoseconds. Below temperatures of  $180$ – $220$  K, those motions vanish that have diffusive character. In the case of

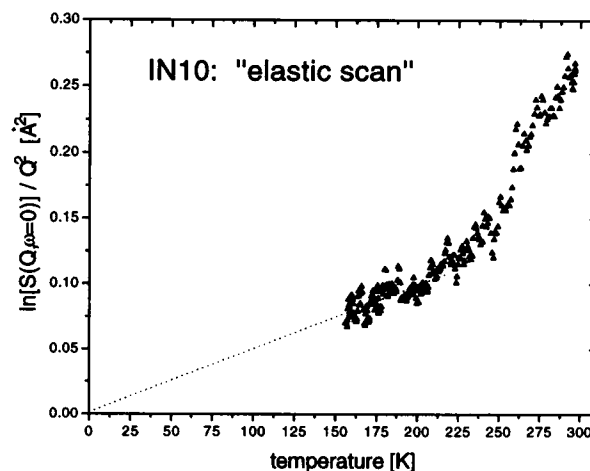


FIGURE 4 The temperature dependence of the average mean square displacements as obtained from an "elastic scan" measured with IN10. The average mean square displacements ( $\langle u^2 \rangle$ ) have been derived by using  $S_{\text{inc}}(\vec{Q}, \omega = 0) \propto e^{-\langle u^2 \rangle Q^2}$ , which includes all diffusive as well as vibrational motions with correlation times smaller than  $300$  ps. The straight line represents an assumed linear temperature dependence of the average mean square displacements below  $200$  K, corresponding to (harmonic) vibrational motions in this temperature range. Note that this kind of analysis also reveals the relevant features of temperature dependence at higher temperatures, which is mainly represented by the temperature dependence of  $\text{QISF}_2$  and  $\text{QISF}_1$  shown in Fig. 3, B and C.

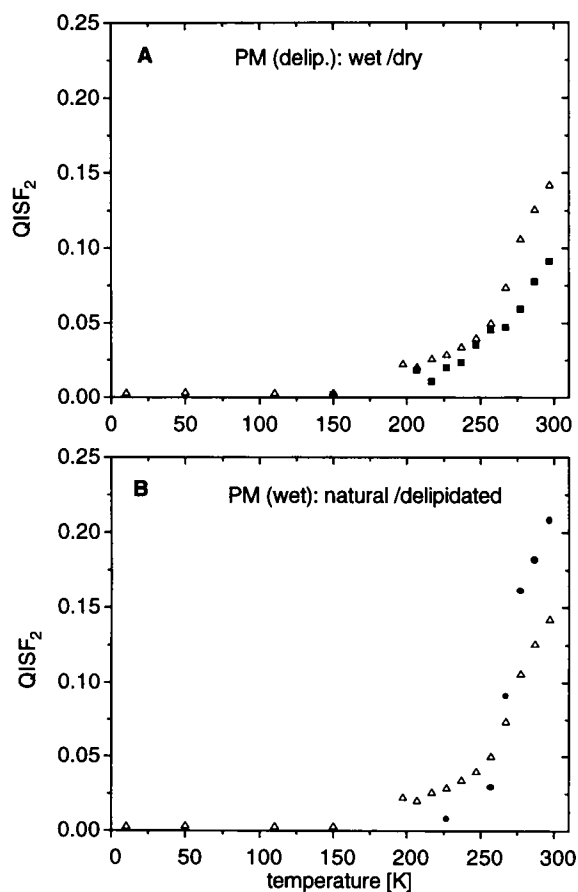


FIGURE 5 Quasielastic incoherent structure factors of PM samples at different conditions. (a)  $\text{QISF}_2$  of delipidated PM, fully hydrated with  $h = 0.38 \text{ g D}_2\text{O/g PM}$  ( $\Delta$ ) and weakly hydrated with  $h = 0.18 \text{ g D}_2\text{O/g PM}$  ( $\blacksquare$ ). (b)  $\text{QISF}_2$  of fully hydrated samples of delipidated PM ( $\Delta$ ) and of natural PM ( $\bullet$ ).

fully hydrated samples, there is an additional reduction in thermal fluctuations (between 270 K and 260 K) resulting from the crystallization of hydration water. The scattering component representing the faster motions (with correlation times smaller than 0.2 ps) seems to include diffusive and vibrational motions. The analysis of spectra at lower  $Q$  values ( $Q = 1.2\text{--}1.6 \text{ \AA}^{-1}$ ) shows a very similar behavior, with vanishing diffusive motions below 180–220 K.

Although we focus mainly on the fact that the motions are purely vibrational below 180–220 K, in contrast to predominantly diffusive motions above this temperature, we also want to comment briefly on the question of harmonicity of the vibrational motions. A linear dependence of mean square displacements on the temperature is evidence for a parabolic energy potential, which gives rise to harmonic vibrational motions. Because our data are not really complete at low temperatures (see Figs. 3 C and 4), we are not able to prove a pure linearity of mean square displacements with the temperature. It seems reasonable to assume, however, that the motions are close to harmonic in this temperature regimen.

## THE DEPENDENCE ON HYDRATION LEVEL

The dynamical properties have been studied as a function of hydration level by measuring natural PM samples hydrated at levels ranging from 0.05 to 0.56 g  $\text{D}_2\text{O/g PM}$ . These measurements were performed at room temperature with NEAT, with an elastic energy resolution of  $\Delta E = 100 \mu\text{eV}$ . As in the procedure applied for studying the temperature dependence, we determined the linewidths and quasielastic structure factors of two components with the fully hydrated sample ( $h = 0.56 \text{ g D}_2\text{O/g PM}$ ) and used the obtained linewidths as fixed parameters in the analysis of spectra measured at lower hydration levels. This procedure enabled fits of reasonable quality (Fig. 6) to be obtained. The resulting quasielastic structure factors are shown as a function of hydration level in Fig. 7. The analysis of these fits revealed the following features:

1. “Fast” motions due to the broad component (represented by  $\text{QISF}_1$ ) are not influenced very much by the hydration level. In contrast to this, the “slower” motions (represented by  $\text{QISF}_2$ ) are much more pronounced at high hydration levels than they are at low hydration levels.

2. Even at rather low hydration levels, an appreciable part of slow diffusive motions contributes to the total dynamics. Raising the hydration level, we find a drastic increase in these slower motions (above  $h = 0.3$ ), which seems to be characterized by a saturation above  $h = 0.4$ .

These results suggest that mainly the slow local diffusive motions of molecular subunits located on the surface of the protein-lipid complex are influenced by the solvent molecules. These subunits are affected by surrounding solvent molecules through van der Waals interaction and by screening of electrostatic interaction, which have the effect of an increased flexibility induced in parts of the protein-lipid complex. Additional solvent molecules (leading to  $h \geq 0.4$ ) do not participate in the hydration of the protein-lipid complex, but increase the amount of excess water. Therefore we do not observe an increasing flexibility above a certain value of hydration. On the other hand, quasielastic scattering is clearly resolved, also at very low hydration levels, suggesting that we are observing slow stochastic motions of subunits located in the interior of the protein-lipid complex, which are not much influenced by solvent molecules.

## DISCUSSION

The well-known “dynamical transition” is one of the most important features of the temperature dependence of molecular motions in proteins. Up to now, the physical and chemical details of this transition are not fully understood. Its phenomenological characteristics are found to be very similar in many different proteins, even by different methods. A drastically increased “flexibility” of the protein structure above the transition temperature ( $T_d = 180\text{--}220 \text{ K}$ ) is always observed, even at very different time scales ranging from  $10^{-7} \text{ s}$  (as observed by Mössbauer spectroscopy; Parak et al., 1982), to  $10^{-13} \text{ s}$  (as observed by neutron



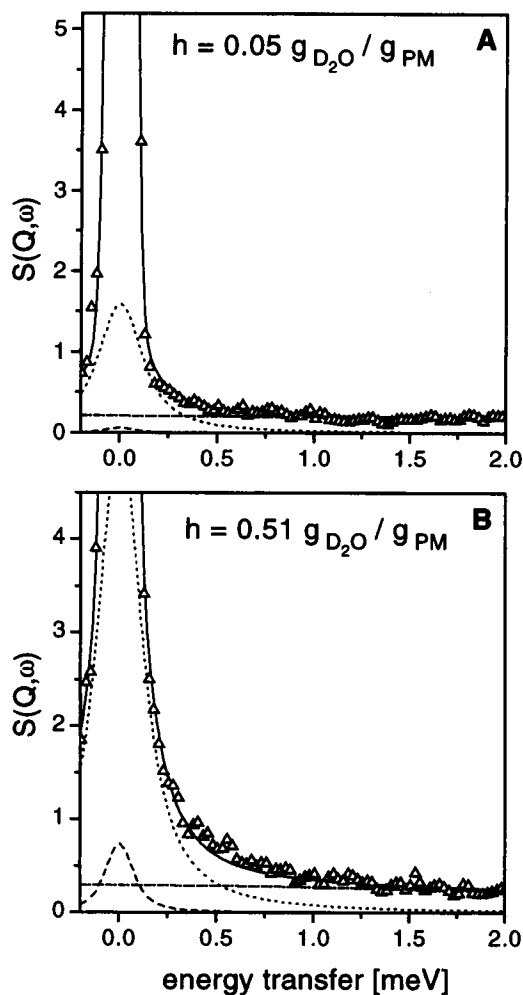


FIGURE 6 The influence of the hydration level on the quasielastic components is shown by fits of NEAT spectra ( $Q = 1.7 \text{ \AA}^{-1}$ ) measured at room temperature. The spectra have been measured with natural PM samples at low hydration level (a) and high hydration level (b). The total scattering function (solid line), which is fitted to the experimental points (triangles), includes the following quasielastic components: scattering from the PM represented by Lorentzian  $L_1$  with  $H_1 = 4 \text{ meV}$  (dashed-dotted line), and  $L_2$  with  $H_2 = 120 \text{ } \mu\text{eV}$  (dotted line). Scattering due to rotational diffusion of  $\text{D}_2\text{O}$  molecules is represented by the dashed line (parameter values; see legend of Fig. 3). The largest intensity values (top of the frame) shown in both figures correspond to 10% of the elastic peak intensity.

spectroscopy; Doster et al., 1989; Ferrand et al., 1993). Furthermore, the increase in “flexibility” is much more pronounced in fully hydrated samples as compared to dry samples. A detailed interpretation of spectroscopic neutron scattering data from biological macromolecules in terms of mean square displacements, jump distances, jump rates, and correlation times is difficult. These parameters and, in particular, their dependence on environmental conditions (temperature and hydration) often cannot be determined unambiguously (see The Temperature Dependence, above). Using the Gaussian approximation, one obtains global mean-square displacements characterizing the combined ef-

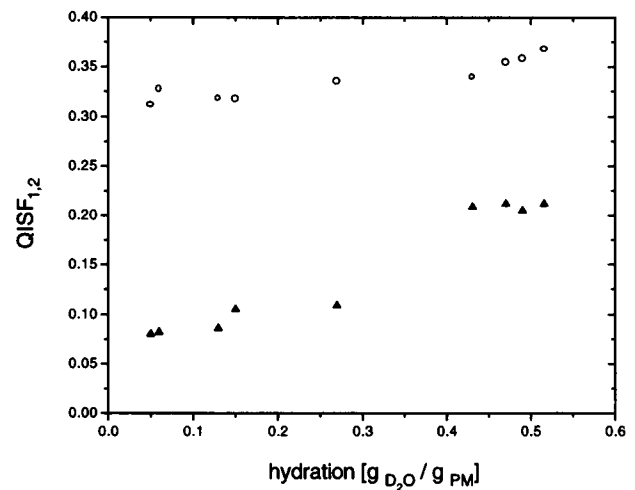


FIGURE 7 Two quasielastic structure factors as function of hydration level.  $\text{QISF}_1$  ( $\circ$ ) with  $H_1 = 4 \text{ meV}$  is related to faster motions, whereas  $\text{QISF}_2$  ( $\blacktriangle$ ) with  $H_2 = 120 \text{ } \mu\text{eV}$  represents the slower motions.

fect of all types of motions that are faster than those corresponding to a certain correlation time determined by the energy resolution of the measurement. Comparing our IN10 data (see Fig. 4) with data measured by Ferrand et al., (1993) for IN13 ( $\Delta E = 10 \text{ } \mu\text{eV}$  (full width half-maximum; FWHM)) and using a similar PM sample, we find mean square displacements for the IN10 data, which are larger by a factor of 2 to 3 than those from IN13. (To compare the values given in this paper with the IN13 data, divide the mean square displacements of the latter (Ferrand et al. 1993) by a factor of 3, because the authors used another definition of  $\langle u^2 \rangle$ .) This is due to the better energy resolution of IN10 as compared to IN13. Apart from this, the qualitative features of the temperature dependences are rather similar. A more detailed study of the individual temperature dependences of motions in different time protocols requires the analysis of the whole spectra and measurements at different energy resolutions. Such an analysis, presented in this paper, revealed that broad components corresponding to faster motions with correlation times smaller than 0.2 ps are not exclusively diffusive, but also include an appreciable amount of vibrational motion, which does not vanish immediately below the transition temperature. In this context the question of how the individual motions are affected by lowering the temperature is of fundamental interest. A description of the dynamical transition, using mean-square displacements as a function of temperature, suggests that the required volume or the jump distances of the motions are decreasing with decreasing temperature. Such an interpretation was given in a study of superoxide dismutase by Andreani and co-workers (1995). Furthermore, these authors found, with decreasing temperature, a  $T$ -independent linewidth ( $24 \text{ } \mu\text{eV}$  (half-width half-maximum; HWHM) recorded with an elastic energy resolution of  $15 \text{ } \mu\text{eV}$  (FWHM) within an energy transfer range of  $\pm 0.5 \text{ meV}$ ) of a quasielastic component with decreasing intensity, which

was related to decreasing volumes explored by the individual motions. In a study on the dynamical transition of myoglobin, Doster and co-workers (1989) separated two quasielastic components using data obtained from measurements with IN13 ( $\Delta E = 10 \mu\text{eV}$  (FWHM)) and IN6 ( $\Delta E = 80 \mu\text{eV}$  (FWHM)). These authors report that a broad component (linewidth of 1.5–2.0 meV) shows a  $T$ -independent linewidth, whereas the linewidth of the other component (related to slower motions) broadens with increasing temperature. The linewidths obtained by these authors, characterizing individual motions occurring in the samples, seem to depend strongly on the energy resolution and energy transfer range of the analyzed measurements. Nevertheless, from the phenomenological point of view, all above-mentioned studies of the temperature dependences of myoglobin, superoxide dismutase, and BR give very similar results, as compared to those for BR in this paper as well as in previous studies (Fitter et al., 1996a). But as reported in the present work, the approach of relating decreasing quasielastic scattering components to decreasing “amplitudes” of the motions is only one possible interpretation. Another one is that the motions become slower with decreasing temperature. According to the model introduced by Frauenfelder and co-workers (1979), diffusive motions are related to “barrier crossing” between conformational substrates, and reduced jump rates at lower temperatures may appear more plausible than the idea of decreasing the jump distances. (This is also supported by the fact that the three-dimensional structure of proteins, which determines the energy landscape, is not significantly changed at low temperatures as compared to room-temperature structures.) In this picture, the “amplitudes” of moving subunits may become smaller only in the sense that below a certain temperature the diffusive motions vanish and we only observe vibrational motions restricted by potential barriers, which results in much smaller apparent “amplitudes.” Indeed, below  $\sim 200$  K, we do not find quasielastic scattering in the spectra. On the other hand, the dynamical properties of the hydration water, which are also  $T$ -dependent, showing increasing reorientation rates with increasing temperatures, are strongly related to the energy landscape of the protein structure (Singh et al., 1981). In contrast to low temperatures, at higher temperatures hydration water is able to lower the energy barriers, which may cause not only higher jump rates but also larger jump distances (Pethig, 1992; Rupley and Careri, 1991). Nevertheless, even with combined data from spectra measured at different energy resolutions, it has so far not been possible to deduce unambiguously whether the relaxational processes are generally slowed down or whether the spatial extension of the motion is reduced by lowering the temperature. Although the studies of other authors, cited above, have been performed with different proteins, it can be assumed that the discussed dynamical characteristics are general properties of all proteins, or even of all biological macromolecules.

In addition to the temperature, the degree of hydration is also a relevant parameter that has a strong influence on the

characteristics of the dynamical properties of proteins and on the dynamical transition. We find an influence of the hydration level on the dynamical behavior (described by motions with correlation times of a few picoseconds; see Fig. 5 A) only at temperatures higher than  $T_f$ . Previous investigations on purple membranes (Ferrand et al., 1993), on superoxide dismutase (Andreani et al., 1995), and on L- $\alpha$  dipalmitoylphosphatidylcholine multilayers (König et al., 1995) show significant differences of the average mean square displacements and of quasielastic structure factors between wet and dry samples above temperatures of 200–220 K. When the dynamical behavior of the PM is compared as a function of temperature and as a function of hydration level, the two parameters have rather different effects on the dynamical behavior. In contrast to low temperatures, where the slower motions ( $\tau \geq 5$  ps) really vanish, these motions were still observed to an appreciable extent at rather low hydration levels. Furthermore, the faster motions ( $\tau \approx 0.2$  ps) are not influenced very much by a decreasing hydration level, but they are significantly reduced by lowering the temperature.

The results obtained in the present investigation support the idea that hydrogen bond networks play an essential role in the dynamical transition. Relative to covalent and ionic bonds, which are also present in protein structures, hydrogen bonds are rather weak and can be transiently formed and broken because of the thermal energy fluctuations occurring at physiological temperatures. At sufficient hydration, the presence of numerous water molecules in the vicinity of polypeptide side groups is related to many alternative hydrogen bonds between polypeptide side groups and different water molecules. These hydrogen bonds have comparable energy and similar probability, which permits structural flexibility of the protein due to large amplitude stochastic fluctuations (see for example Rupley and Careri, 1991; Pethig, 1992). Limiting factors in this process are a sufficient number of solvent molecules and temperatures high enough to enable forming and breaking of alternative hydrogen bonding arrangements. A further increase in the temperature leads to higher reorientation rates or larger “amplitudes.” (In general, even higher temperatures (above 330 K) may cause the denaturation of water-soluble proteins accompanied by the unfolding of the tertiary structure, demonstrating that hydrogen bonds in protein structures play another important role: the stabilization of the three-dimensional structure at physiological conditions (Myers and Pace, 1996).) In contrast to this, the addition of further solvent molecules ( $h \geq 0.4$ ) is not related to an additional increase in flexibility within the protein. In the case of BR, which is embedded in lipids, the protein has many hydrophobic polypeptide side groups on its surface contacting the hydrophobic chains of the lipids. Although the lipid headgroups in particular are supposed to play an important role in the hydration of the PM (Zaccai, 1987), which is also related to internal motions inside the PM (Fitter et al., 1997), hydrophobic groups should be less influenced by the network of hydrogen bonds. This is probably the reason

why we still find some reorientational motions, even at low hydration levels.

Finally, we want to discuss the dynamical properties in relationship to the function of BR as a proton pump. The effects of lowering the temperature and lowering the hydration level as compared to samples at physiological conditions are rather similar in many respects. In both cases a decreasing decay rate of the M-intermediate and, related to this, a reduced  $H^+$ -pump activity are observed. In fully hydrated samples, the decay rate of the M-intermediate becomes extremely small below temperatures of  $\sim 180$ – $200$  K (Iwasa et al., 1980). At room temperature proton pumping is drastically reduced below hydration levels of about  $h = 0.13$ – $0.15$  (Korenstein and Hess, 1977; Thiedemann et al., 1992). (A hydration level of 0.15 is achieved in samples that are hydrated at 75% relative humidity.) The latter is accompanied by the disappearance of conformational changes in the tertiary structure below the hydration level given above (Sass et al., 1997). The observed transition from supercooling to crystallization of parts of the hydration water at  $T_f$ , resulting in an effective dehydration of the samples (see The Temperature Dependence), gives rise to the following question: Is the cooling itself, or is the resulting dehydration the reason that BR is missing its functional properties at low temperatures; or is it a combination of both? Nevertheless, the observations suggest that the picosecond dynamics studied in the present paper is related to the photoinduced processes (e.g., late intermediates of the photocycle, vectorial proton transfer, conformational changes) occurring on the microsecond to millisecond time scale. Qualitatively we find that decreasing protein activity is accompanied by a decreasing internal flexibility of the protein on the picosecond time scale. But up to now we are not able to find detailed indications of how the features of the picosecond dynamics are linked to the features or key events of the protein working process. In the particular case of BR, the following questions concerning this subject are of special interest: Is the dynamical transition responsible for the onset of proton pumping above 180–200 K? Water molecules serve the proton pump BR as a solvent to hydrate the protein and to ensure a sufficient internal flexibility. In addition, water molecules are found to be a part of a proton pathway inside the protein (Papadopoulos et al., 1990), which is supposed to be functionally important for the vectorial proton transfer across the membrane (Nagel et al., 1983; Dencher et al., 1992). Which of these two roles of water molecules is the limiting factor of proton pump activity at low hydration levels? Answering these questions will require further experiments and a combination of techniques investigating the dynamical aspects of both the "overall" structure (neutron spectroscopy) and important functional local sites (label techniques).

## CONCLUSION

Using measurements with three different elastic energy resolutions, we analyzed local diffusive motions occurring in

the protein-lipid complex of purple membrane. The correlation times of these motions exhibit a broad quasicontinuous distribution, ranging from 0.1 to a few hundred picoseconds. Within the whole range of this time regime, a dynamical transition, characterized by the onset of local diffusive motions, appears between temperatures of 180 K and 220 K. The hydration level of the purple membranes affects mainly motions with correlation times slower than a few picoseconds. In contrast to the temperature dependence, faster motions are not much influenced by the level of hydration. A transition from supercooling to crystallization of hydration water (at  $T \approx 267$  K) in samples with moderate (physiological) hydration levels ( $h > 0.2$ ) exhibits a strong correlation between temperature and hydration level, which is also reflected in the dynamical behavior of the protein-lipid complex. This observation is relevant for many investigations of the functional properties of BR at low temperatures.

We thank O. Randl and M. Ferrand (ILL, Grenoble) for their assistance as local contacts during the IN10 and IN6 experiments. We are very much indebted to G. Büldt for many stimulating discussions and continuous support.

This work was supported by grant 03-DE4DAR-1 from Bundesministerium für Forschung und Technologie.

## REFERENCES

- Andreani, C., A. Filabozzi, F. Menzinger, A. Desideri, A. Deriu, and D. Di Cola. 1995. Dynamics of hydrogen atoms in superoxide dismutase by quasielastic neutron scattering. *Biophys. J.* 68:2519–2523.
- Dencher, N. A., G. Büldt, J. Heberle, H.-D. Höltje, and M. Höltje. 1992. Light-triggered opening and closing of a hydrophobic gate controls vectorial proton transfer across bacteriorhodopsin. In *Proton Transfer in Hydrogen-Bonded Systems*. T. Bountis, editor. Plenum Press, New York, 171–185.
- Dencher, N. A., D. Dresselhaus, G. Zaccai, and G. Büldt. 1989. Structural changes in bacteriorhodopsin during proton translocation revealed by neutron diffraction. *Proc. Natl. Acad. Sci. USA.* 90:9668–9672.
- Doster, W., A. Bachleitner, R. Dunau, M. Hiebl, and E. Lüscher. 1986. Thermal properties of water in myoglobin crystals and solutions at subzero temperatures. *Biophys. J.* 50:213–219.
- Doster, W., S. Cusack, and W. Petry. 1989. Dynamical transition of myoglobin revealed by inelastic neutron scattering. *Nature.* 337: 754–756.
- Ferrand, M., A. J. Dianoux, W. Petry, and G. Zaccai. 1993. Thermal motions and function of bacteriorhodopsin in purple membranes: effects of temperature and hydration studied by neutron scattering. *Proc. Natl. Acad. Sci. USA.* 90:9668–9672.
- Fitter, J. 1994. Untersuchung der molekularen Dynamik in Purpormembranen mit quasielastisch inkohärenter Neutronenstreuung. Ph.D. thesis. Freie Universität Berlin, Berlin.
- Fitter, J., M. Adams, G. Coddens, G. Büldt, N. A. Dencher, and R. E. Lechner. 1995. Dynamical structure and function of purple membrane as seen by neutrons. *Physica B.* 213/214:775–779.
- Fitter, J., R. E. Lechner, G. Büldt, and N. A. Dencher. 1996a. Temperature dependence of molecular motions in the membrane protein bacteriorhodopsin from QINS. *Physica B.* 226:61–65.
- Fitter, J., R. E. Lechner, N. A. Dencher, and G. Büldt. 1996b. Internal molecular motions of bacteriorhodopsin: hydration-induced flexibility studied by quasielastic incoherent neutron scattering using oriented purple membranes. *Proc. Natl. Acad. Sci. USA.* 93:7600–7605.

- Fitter, J., R. E. Lechner, and N. A. Dencher. 1997. Influence of lipids on the dynamical behavior of bacteriorhodopsin in the purple membrane. *J. Biomol. Struct. Dyn.* (in press).
- Frauenfelder, H., G. A. Petsko, and D. Tsernoglou. 1979. Temperature-dependent x-ray diffraction as a probe of protein dynamics. *Nature*. 280:558–563.
- Grigorieff, N., T. A. Ceska, K. H. Downing, and R. Henderson. 1996. Electron-crystallographic refinement of the structure of bacteriorhodopsin. *J. Mol. Biol.* 259:393–421.
- Hauss, T., G. Büldt, M. P. Heyn, and N. A. Dencher. 1994. Light-induced isomerization causes an increase in the chromophore tilt in the M intermediate of bacteriorhodopsin: a neutron diffraction study. *Proc. Natl. Acad. Sci. USA*. 91:11854–11858.
- Henderson, R., J. M. Baldwin, T. A. Ceska, F. Zemlin, E. Beckmann, and K. H. Downing. 1990. Model for the structure of bacteriorhodopsin based on high-resolution electron cryo-microscopy. *J. Mol. Biol.* 213: 899–929.
- Iben, I. E. T., D. Braunstein, W. Doster, H. Frauenfelder, M. K. Hong, J. B. Johnson, S. Luck, P. Ormos, A. Schulte, P. J. Steinbach, A. H. Xie, and R. D. Young. 1989. Glassy behavior of a protein. *Phys. Rev. Lett.* 62:1916–1919.
- Iwasa, T., F. Tokunaga, and T. Yoshizawa. 1980. A new pathway in the photoreaction cycle of trans-bacteriorhodopsin and the absorption spectra of its intermediates. *Biophys. Struct. Mech.* 6:253–270.
- Kates, M., S. C. Kushwaha, and G. D. Sprott. 1982. Lipids of purple membrane from extreme halophiles and methanogenic bacteria. *Methods Enzymol.* 88:98–111.
- Koch, M. H., N. A. Dencher, D. Oesterhelt, H.-J. Plöhn, G. Rapp, and G. Büldt. 1991. Time resolved x-ray diffraction study of structural changes associated with the photocycle of bacteriorhodopsin. *EMBO J.* 10: 521–526.
- König, S., T. M. Bayerl, G. Coddens, D. Richter, and E. Sackmann. 1995. Hydration dependence of chain dynamics and local diffusion in L- $\alpha$ -dipalmitoylphosphatidylcholine multilayers studied by incoherent quasielastic neutron scattering. *Biophys. J.* 68:1871–1880.
- Korenstein, R., and B. Hess. 1977. Hydration effects on the photocycle of bacteriorhodopsin in thin layers of purple membrane. *Nature*. 270: 184–186.
- Kuntz, I. D., and W. Kauzmann. 1974. Hydration of proteins and polypeptides. *Adv. Protein Chem.* 28:239–345.
- Landolt-Börnstein, H. Borchers, H. Hausen, K. H. Hellwege, K. Schaefer, and E. Schmidt, editors. 1967. Zahlenwerte und Funktionen. IV. Band Technik. 4. Teil Wärmetechnik. Springer-Verlag, Berlin.
- Lechner, R. E. 1983. Neutron scattering studies of diffusion in solids. In *Mass Transport in Solids*. F. Beniere and C. R. A. Catlow, editors. Plenum, New York. 169–226.
- Lechner, R. E. 1994. Structural aspects of diffusive motion in some complex systems. In *Quasielastic Neutron Scattering: Future Prospects on High-Resolution Inelastic Neutron Scattering*. J. Colmenero, A. Alegria, and F. J. Bermejo, editors. World Scientific, Singapore. 62–91.
- Lechner, R. E., N. A. Dencher, J. Fitter, G. Büldt, and A. V. Belushkin. 1994a. Proton diffusion on purple membrane studied by neutron scattering. *Biophys. Chem.* 49:91–99.
- Lechner, R. E., N. A. Dencher, J. Fitter, and Th. Dippel. 1994b. Two-dimensional proton diffusion on purple membrane. *Solid State Ionics*. 70/71:296–304.
- McCammon, J. A., and S. C. Harvey. 1987. *Dynamics of Proteins and Nucleic Acids*. Cambridge University Press, Cambridge.
- Myers, J. K., and C. N. Pace. 1996. Hydrogen bonding stabilizes globular proteins. *Biophys. J.* 71:2033–2039.
- Nagel, J. F., and S. Tristram-Nagel. 1983. Hydrogen bonded chain mechanisms for proton conduction and proton pumping. *J. Membr. Biol.* 74:1–14.
- Y. A. Ovchinnikov, N. G. Abdulaev, M. Y. Feigina, A. V. Kiselev, and N. A. Lobanov. 1979. The structural basis of the functioning of bacteriorhodopsin: an overview. *FEBS Lett.* 100:219–224.
- Papadopoulos, G., N. A. Dencher, G. Zaccai, and G. Büldt. 1990. Water molecules and exchangeable hydrogen ions at the active centre of bacteriorhodopsin localized by neutron diffraction. *J. Mol. Biol.* 214: 15–19.
- Parak, F., and H. Frauenfelder. 1993. Protein dynamics. *Physica A*. 201: 332–345.
- Parak, F., E. W. Knapp, and D. Kucheida. 1982. Mössbauer spectroscopy on desoxyhemoglobin crystals. *J. Mol. Biol.* 161:177–194.
- Pethig, R. 1992. Protein-water interactions determined by dielectric methods. *Annu. Rev. Phys. Chem.* 43:177–205.
- Rupley, J. A., and G. Careri. 1991. Protein hydration and function. *Adv. Protein Chem.* 41:37–172.
- Sass, H. J., I. Schachowa, G. Rapp, M. H. J. Koch, D. Oesterhelt, G. Büldt, and N. A. Dencher. 1997. Tertiary structural changes in bacteriorhodopsin occur between M substrates: x-ray diffraction and Fourier transform infrared spectroscopy. *EMBO J.* (in press).
- Singh, G. P., F. Parak, S. Hunklinger, and K. Dransfeld. 1981. Role of adsorbed water in the dynamics of metmyoglobin. *Phys. Rev. Lett.* 47:685–688.
- Thiedemann, G., J. Heberle, and N. A. Dencher. 1992. Bacteriorhodopsin pump activity at reduced hydration. In *Structures and Functions of Retinal Proteins*. J. L. Rigaud, editor. Libbey Eurotext. Montrouge, France. 217–220.
- Van Hove, L. 1954. Correlations in space and time and Born approximation scattering in systems of interacting particles. *Phys. Rev.* 95: 249–262.
- Varo, G., and L. Keszthelyi. 1983. Photoelectric signals from dried oriented purple membranes of *Halobacterium halobium*. *Biophys. J.* 43: 47–51.
- Zaccai, G. 1987. Structure and hydration of purple membranes in different conditions. *J. Mol. Biol.* 194:569–572.